

Angular dependence of the high-frequency vortex response in $\text{YBa}_2\text{Cu}_3\text{O}_{7-x}$ thin film with self-assembled BaZrO_3 nanorods

N. Pompeo^{a,*}, R. Rogai^a, K. Torokhtii^a, A. Augieri^b, G. Celentano^b, V. Galluzzi^b, E. Silva^a

^aDipartimento di Fisica "E. Amaldi" and Unità CNISM, Università Roma Tre, Via della Vasca Navale 84, 00146 Roma, Italy

^bENEA-Frascati, Via Enrico Fermi 45, 00044 Frascati, Roma, Italy

Abstract

We present a microwave study of the angular dependence of the flux-flow resistivity ρ_{ff} and of the pinning constant k_p in YBCO thin films containing BZO nanorods. We find that BZO nanorods are very efficient pinning centers, even in tilted fields. We find that ρ_{ff} is a scaling function of a reduced field $H/f(\theta)$. We extend a model for the anisotropic motion of vortices in uniaxially anisotropic superconductor, able to describe the experimental $f(\theta)$ on the basis of only the intrinsic anisotropy of YBCO. The pinning constant k_p , by contrast, exhibits different field dependences in different angular ranges, consistent with pinning by BZO at angles as large as 60° , and with pinning along the a, b planes as originating from the same mechanism as in pure YBCO with the field along the c axis.

Keywords: YBCO, BaZrO_3 nanorods, surface impedance, vortex dynamics, angular dependence

1. Introduction and model

Enhanced pinning by artificial defects, such as those originated by BaZrO_3 (BZO) inclusions within $\text{YBa}_2\text{Cu}_3\text{O}_{7-x}$ (YBCO) films, has been extensively studied in the last years due to the potential impact on applications, with substantially increased critical currents and irreversibility fields [1, 2, 3]. Issues connected to the directional nature of the pinning efficiency have been under careful scrutiny, since BZO defects self-assemble typically in linear structures roughly parallel to the c axis, thus competing with intrinsic pinning due to the layered structure itself. As a consequence, the angular dependence of critical current density j_c is heavily affected by BZO defects [1, 4], with a maximum of j_c along the c axis. Whether this behaviour competes or coexists with the intrinsic anisotropy of YBCO is difficult to ascertain with a dc technique, where the pinning potential is probed at high current densities, that is when the flux lines can be extracted from the pinning potential wells and moved apart.

We present in this paper a microwave study of the angular dependence of the vortex motion resistivity in a YBZO/BZO film, where we disentangle the effects

of directional pinning from the intrinsic anisotropic resistivity, exploiting the peculiarities of the microwave complex response. At microwave frequencies the flux lines oscillate over distances of less than ~ 1 nm [5], thus probing only the bottom (i.e., the steepness) of the pinning potential. Interestingly, we observed previously a strong increase of pinning as measured at ~ 50 GHz in YBCO/BZO films with different BZO content [6], thus showing that BZO induces very steep pinning wells. The short-distance oscillations allow in most cases the application of mean-field theories developed for the vortex motion resistivity ρ_{vm} [7, 8, 9]. Comparison with the data is made easier by the fact that those theories can be described by a unified formulation [10]:

$$\rho_{vm} = \rho_{vm,1} + i\rho_{vm,2} = \rho_{ff} \frac{\varepsilon + i(\nu/\bar{\nu})}{1 + i(\nu/\bar{\nu})} \quad (1)$$

where the resistivity ρ_{ff} represents the genuine flux flow resistivity (only viscous drag), reached at high frequency instead of at high currents, $\bar{\nu}$ is a characteristic frequency and the dimensionless parameter $0 \leq \varepsilon \leq 1$ is a measure of thermal activation phenomena. When ε is small, the model reduces to the well-known Gittleman-Rosenblum model [7] and $\bar{\nu} \rightarrow k_p \rho_{ff} / \Phi_0 B$. A complete discussion on the extraction of the vortex parameters k_p (pinning constant) and ρ_{ff} , together with the assessment of the validity limits, has been given in [10]. In the measurements of the angular and field dependence of ρ_{ff}

*Corresponding author.

Email address: pompeo@fis.uniroma3.it (N. Pompeo)

and k_p here reported, the systematic (not scattering) error is less than 20%.

The flux-flow resistivity, as an intrinsic property of superconductors, is a model-dependent function [11, 12, 13] of the reduced field $h = H/H_{c2}$ (in the London approximation, where $B \simeq \mu_0 H$), $\rho_{ff} = \rho_n F(h)$, where ρ_n is the normal state resistivity. The Bardeen-Stephen (BS) model [13] predicts linearity with the field, $\rho_{ff} = \rho_n h$. When H is tilted by an angle θ from the c axis, H_{c2} acquires an angular dependence: $H_{c2}(\theta) = H_{c2}(0)\epsilon(\theta)$, with $\epsilon(\theta) = [\cos^2 \theta + \gamma^{-2} \sin^2 \theta]^{1/2}$ in the anisotropic 3D Ginzburg-Landau model, with $\gamma = H_{c2}(0^\circ)/H_{c2}(90^\circ) \simeq 5 \div 8$ in YBCO. The resulting flux flow resistivity becomes

$$\rho_{ff}(H, \theta) = \rho_n H / H_{c2}(0^\circ) \epsilon(\theta) \quad (2)$$

In dc, Eq. 2 holds for the genuine flux flow resistivity, and when the force acting on flux lines does not change with the angle: this is typically the case when pinning is irrelevant or isotropic (e.g. in the crossover region between the flux-flow and fluctuation regimes [14]) and the Lorentz force on flux lines is constant. When directional pinning plays a role, the scaling hypothesis for the measured resistivity breaks down: a scaling (ρ_{ff}) and a non-scaling (pinning force) quantities mix to give the observed total vortex motion resistivity $\rho_{vm} \neq \rho_{ff}$, so that a comprehensive description of the experiments becomes difficult.

A second issue, relevant to this paper, comes when the angle between H and the current is varied. In this case the driving force changes with the angle. On a theoretical ground, this is far from being a trivial problem, and a general expression for ρ_{ff} can be written only under restrictive assumptions. Using a time-dependent Ginzburg Landau approach, Hao, Hu and Ting (HHT) [15] have obtained an expression for the flux flow resistivity in anisotropic superconductors. In spherical coordinates, where $c \parallel z$, θ is the angle of H with z and ϕ is the angle between x and the in-plane projection of H , in a uniaxial superconductor with $J \parallel x$ we reduce the HHT expression to:

$$\rho_{ff}(\theta, \phi) = \rho_{ab}(\theta) \frac{\rho_{ab}(\theta) \sin^2 \theta \sin^2 \phi + \rho_c(\theta) \cos^2 \theta}{\rho_{ab}(\theta) \sin^2 \theta + \rho_c(\theta) \cos^2 \theta} \quad (3)$$

where ρ_{ab}, ρ_c are the intrinsic a, b plane and c axis flux flow resistivity,¹ and ρ_{ff} stands for the experimentally measured, in-plane flux flow resistivity. When (i) the

¹While $\rho_{ab}(\theta)$ can be directly measured when $\phi = 0$, see Eq.(3), $\rho_c(\theta)$ can be derived (see [15] for extensive discussion) only with a multiterminal technique (such as, e.g., in [16]).

anisotropic scaling applies, (ii) the flux flow resistivities are linear with the field (BS model), and (iii) $\rho_{c,n}/\rho_{ab,n} \simeq \gamma^2$, we obtain

$$\rho_{ff}(\theta, \phi) = \rho_{ab}(\theta = 0) \frac{\gamma^{-2} \sin^2 \theta \sin^2 \phi + \cos^2 \theta}{(\gamma^{-2} \sin^2 \theta + \cos^2 \theta)^{1/2}} \quad (4)$$

Eq. (4) is obtained under strong restrictions (in particular, (iii) is only approximate, even if the order of magnitude is correct [17, 18]). Nonetheless, in nearly optimally doped or overdoped YBCO we do not expect significant deviations from the assumptions (i)-(iii). In Sec. 3 we will compare an extension of Eq. (4) to our anisotropic data for ρ_{ff} .

2. Experimental section

We hereby analyze a YBCO/BZO sample grown by PLD from targets containing BaZrO₃ (BZO) powders at 5% mol. (details are extensively given in [19]). The BZO inclusions generated columnar-like defects, approximately perpendicular to the film plane, as observed with transverse TEM images [20]. The directionality of the defects is consistent with the angular dependence of the critical current density [4].

The complex microwave effective surface impedance has been measured by a sapphire cylindrical dielectric resonator operating at ~ 48 GHz, extensively described elsewhere [21], so that we report here only the results. For the discussion of the data, it is important to stress that the microwave currents J_{mw} flow parallel to the film plane (i.e. parallel to the a, b planes) on a circular fashion (see inset of Fig. 1). A dc magnetic field $\mu_0 H \leq 0.8$ T was applied at the angle θ with the c axis. Field sweeps were performed at different angles. We verified that the angular response was symmetric with respect to the a, b planes. The raw data yielded $\Delta\rho(H)/d = [\rho(H) - \rho(0)]/d = [\Delta\rho_1 + i\Delta\rho_2]/d$, where $\rho = \rho_1 + i\rho_2$ is the complex resistivity and d is the film thickness. When T is sufficiently below T_c one can neglect the field-induced pair-breaking. Thus, the subtraction of the zero-field value allows one to identify $\Delta\rho$ with ρ_{vm} . Taking into account this requirement and the disappearance of the signal in the noise as $\theta \rightarrow 90^\circ$ at low T , measurements were performed at $T = 81$ K as a compromise to obtain a reasonable signal for all orientations.

Fig. 1 reports the field dependence of $\Delta\rho_1/d$ and $\Delta\rho_2/d$ for several angles θ . As expected, $\Delta\rho(H)$ decreases with increasing angle, due to the intrinsic anisotropy of YBCO and to the reduced effect of the Lorentz force on flux lines (when $\theta = 0$, $H \perp J_{mw}$,

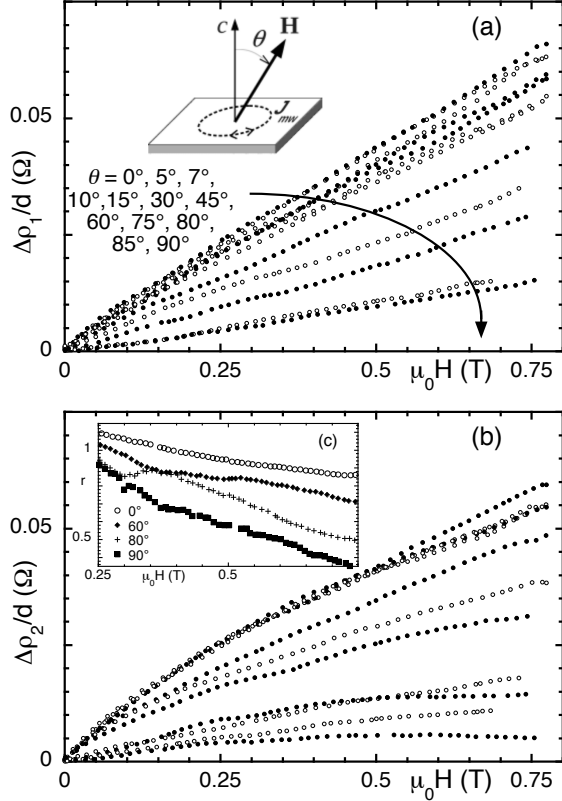


Figure 1: Field induced variation of the real (a) and imaginary (b) microwave resistivity at $T = 81$ K and different angles θ between the dc field and the c axis. For the sake of readability, only a subset of the data are reported. The inset of panel (a) sketches the microwave current pattern and the definition of the angle θ . (c) Field dependence of $r = \Delta\rho_2/\Delta\rho_1$ at selected angles and expanded field scale.

while when $\theta = 90^\circ$ only part of the current lines are perpendicular to the field, thus reducing the net effective Lorentz force). The ratio $r = \Delta\rho_2/\Delta\rho_1$ expresses an experimental measure of the balance between reactive and dissipative contributions to the response. Roughly speaking, $r > 1$ indicates strong pinning. Fig. 1c shows that the overall response becomes progressively dominated by the dissipative contribution with $\theta \rightarrow 90^\circ$. This interesting feature, that might suggest peculiar angular dependence of pinning and of ρ_{ff} , requires the explicit dependence of the vortex parameters for a quantitative discussion.

3. Discussion

We first discuss ρ_{ff} . In Fig. 2a we report ρ_{ff} at selected angles as derived from the data [10]. As a matter of fact, we are able to collapse all the curves (an-

gular scaling) with an empirical angular scaling function $f(\theta)$. We report in Fig. 2b the collapsed curves of ρ_{ff} vs $H/f(\theta)$ and the scaling function $f(\theta)$. As it can be seen, the anisotropy $f(90^\circ)/f(0^\circ)=12$ is significantly larger than the commonly accepted values for the intrinsic anisotropy $\gamma = 5 \div 8$. We ascribe this discrepancy to the varying Lorentz force with θ . Since in our experiment the microwave currents have a circular pattern, we average Eq. (4) over ϕ and we obtain

$$\langle \rho_{ff}(\theta, \phi) \rangle_\phi = \rho_{ab}(0^\circ) \frac{\frac{1}{2}\gamma^{-2} \sin^2 \theta + \cos^2 \theta}{(\gamma^{-2} \sin^2 \theta + \cos^2 \theta)^{1/2}} \quad (5)$$

Taking Eq. (2) for ρ_{ab} , one finds again a scaling law, with $1/f(\theta)$ given by the fraction in Eq.(5). This angular function is plotted in Fig. 2c (solid line). The experimental datum point $f(90^\circ) = 12$ fixes $\gamma = 6$, within the range of commonly accepted values. The zero-parameter curve describes the data well. In particular, it recovers the large effective anisotropy. We can thus state that the flux-flow resistivity, as expected, is an intrinsic property dictated only by the electronic anisotropy of YBCO.

We finally comment on the field dependence of k_p . In Fig. 3 we report k_p vs. H at various θ . There is clearly no possibility to collapse the data onto a single curve by simply rescaling the field, as for ρ_{ff} . The field dependence of k_p gives some insight. In particular, different pinning regimes set in, in different angular regions: in the wide region $0^\circ \leq \theta \leq 45^\circ$, k_p is basically constant (a close inspection reveals that k_p increases slightly with the field) and, interestingly, it is almost angle-independent. With $60^\circ \leq \theta \leq 80^\circ$ the field dependence remains the same, but the absolute values shift upward. With further increasing $\theta \geq 85^\circ$, k_p acquires a strong dependence with the field, decreasing quickly as H increases.

Microwave measurements at $\theta = 0^\circ$ showed [6] that a weakly field-increasing k_p was a feature of YBCO/BZO films, as opposed to field-decreasing k_p , that was typical of pure YBCO. By assigning the constant k_p to the effect of BZO, we get that in the present measurements the pinning mechanism is BZO dominated up to (at least) 45° . By contrast, since the field decrease of k_p is typical of pure YBCO, on qualitative grounds the pinning mechanism in fields nearly parallel to the a, b planes in YBCO/BZO looks the same as in pure YBCO, with the magnetic field along the c axis. In this scenario, the highest absolute values of $k_p(90^\circ)$ are presumably due mostly to the anisotropy, while for $60^\circ \leq \theta \leq 85^\circ$ there is an interplay between pinning by BZO and by anisotropy.

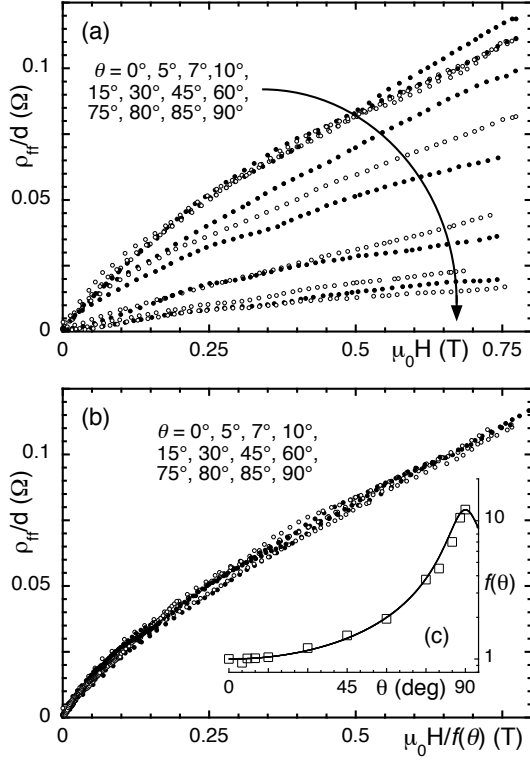


Figure 2: (a) $\rho_{ff}(H)$ at various θ , derived from the measurements of $\Delta\rho$; only 10% of the data have been plotted to avoid crowding. (b) Angular scaling $\rho_{ff}(H/f(\theta))$ for the data in (a). (c) Experimental scaling function $f(\theta)$ (squares) and the anisotropic scaling function corrected with the reduction of the Lorentz force (continuous line) with $\gamma = 6$ (see text); the size of the squares is a measure of the error bars.

4. Summary

We have presented angular measurements of the genuine flux flow resistivity ρ_{ff} and pinning constant k_p in a YBCO film with BZO nanorods. By taking into account the variable Lorentz force in our experimental setup, we have shown that $\rho_{ff}(H, \theta) = \rho_{ff}(H/f(\theta))$, where only the intrinsic H_{c2} anisotropy plays a role. By contrast, k_p shows clear indications of two preferred directions for pinning, ascribed to BZO nanorods and to the a, b planes. The information gained from high-frequency investigations are complementary to dc measurements, since the genuine ρ_{ff} is accessible, and steepness of the pinning potential, rather than the depth, is probed.

We thank S. Schweizer for the help in taking data. This work has been partially supported by the FIRB project “SURE:ARTYST” and by EURATOM. N.P.

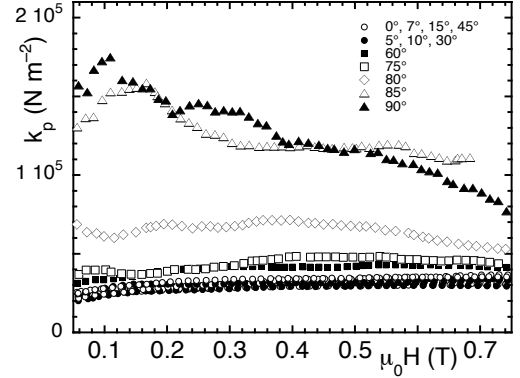


Figure 3: k_p vs. H for the same angles as in Fig. 2; data below $\mu_0 H = 50$ mT are unreliable due to the inversion procedure and are not reported. It is immediately seen that an angular scaling is impossible. Different field dependences, pointing to different pinning mechanisms, develop in different angular regions.

acknowledges support from Regione Lazio.

References

- [1] J. L. Macmanus-Driscoll, S. R. Foltyn, Q. X. Jia, H. Wang, A. Serquis, L. Civale, B. Malorov, M. E. Hawley, M. P. Maley, and D. E. Peterson, Nat. Mater. 3 (2004) 439.
- [2] S. Kang, A. Goyal, J. Li, A. A. Gapud, P. M. Martin, L. Heatherly, J. R. Thompson, D. K. Christen, F. A. List, M. Paranthaman, and D. F. Lee, Science 311 (2006) 1911.
- [3] J. Gutiérrez, A. Llordés, J. Gázquez, M. Gibert, N. Romà, S. Ricart, A. Pomar, F. Sandiumenge, N. Mestres, T. Puig and X. Obradors, Nat. Mater. 6 (2007) 367.
- [4] A. Augieri, V. Galluzzi, G. Celentano, A. Armenio Angrisani, A. Mancini, A. Rufoloni, A. Vannozzi, E. Silva, N. Pompeo, T. Petrisor, L. Ciontea, U. Gambardella, S. Rubanov, IEEE Trans. Appl. Supercond. 19 (2009) 3399.
- [5] W. J. Tomasch, H. A. Blackstead, S. T. Ruggiero, P. J. McGinn, J. R. Clem, K. Shen, J. W. Weber and D. Boyne, Phys. Rev. B 37 (1988) 9864.
- [6] N. Pompeo, R. Rogai, E. Silva, A. Augieri, V. Galluzzi, and G. Celentano, Appl. Phys. Lett. 91, (2007) 182507.
- [7] J. Gittleman and B. Rosenblum, Phys. Rev. Lett. 16 (1966) 734.
- [8] M.W. Coffey and J.R. Clem, Phys. Rev. Lett. 67 (1991) 386.
- [9] E. H. Brandt, Phys. Rev. Lett. 67 (1991) 2219.
- [10] N. Pompeo and E. Silva, Phys. Rev. B 78 (2008) 094503.
- [11] A. I. Larkin and Yu. N. Ovchinnikov, in *Nonequilibrium Superconductivity*, ed. by D. N. Langenberg and A. I. Larkin, 1986, Elsevier, Amsterdam.
- [12] R. J. Troy and A. T. Dorsey, Phys. Rev. B 47 (1993) 2715, and references therein.
- [13] J. Bardeen and M. J. Stephen, Phys. Rev. 140 (1965) A1197.
- [14] S. Sarti, M. Giura, E. Silva, R. Fastampa, V. Boffa, Phys. Rev. B 55 (1997) R6133.
- [15] Z. Hao, C-Ren Hu, C.-S. Ting, Phys. Rev. B 52 (1995) R13138, and references therein.
- [16] M. Esposito, L. Muzzi, S. Sarti, R. Fastampa, E. Silva, J. Appl. Phys. 88 (2000) 2724.
- [17] M. Okuya, T. Kimura, R. Kobayashi, J. Shimoyama, K. Kitazawa, K. Yamafuji, K. Kishio, K. Kinoshita and T. Yamada, J. Supercond. 7 (1994) 313.

- [18] M. Oda, Y. Hidaka, M. Suzuki, and T. Murakami, Phys. Rev. B 38 (1988) 252.
- [19] V. Galluzzi, A. Augieri, L. Ciontea, G. Celentano, F. Fabbri, U. Gambardella, A. Mancini, T. Petrisor, N. Pompeo, A. Rufoloni, E. Silva, and A. Vannozzi, IEEE Trans. Appl. Supercond. 17 (2007) 3628.
- [20] A. Augieri, G. Celentano, V. Galluzzi, A. Mancini, A. Vannozzi, A. Angrisani Armenio, T. Petrisor, L. Ciontea, S. Rubanov, E. Silva, N. Pompeo, J. Appl. Phys. 108 (2010) 063906.
- [21] N. Pompeo, R. Marcon, E. Silva, J. Supercond. and Novel Magnetism 20 (2007) 71.